Materials Physics and Mechanics 46 (2020) 182-190 Received: February 26, 2020

MATERIAL BEHAVIOUR DURING A COMPLEX STRESS TEST OF THIN-WALLED, CYLINDRICAL SINGLE-CRYSTAL SPECIMENS

Boris Vasilyev[1,2*], Alexander Selivanov[1,2], Sergey Shibaev[1]

[1]CIAM, Moscow, 2, Aviamotornaya St., Russia

[2]BMSTU, Moscow, 5, Baumanskaya 2-ya St., Russia

*e-mail: bevasilev@ciam.ru

Abstract. The von Mises and Hill yield criteria are commonly used when the stress-strain state of parts under complex loading conditions is calculated. However, those yield criteria are not suitable in some materials and do not reliably describe the inelastic behavior of the material under complex stress conditions. The development of a simple and accurate criterion of plastic flow is relevant. This paper presents the results of the yield criterion development for a single crystal nickel-based superalloy (ZhS32) based on the systematization of experimental data. Various types of stress state were realized during the experiment: tension, compression, torsion, as well as combinations of tension-torsion, compression-torsion.

Keywords: single-crystal, crystallographic orientation, anisotropy, stress-strain state, plasticity, yield strength, ultimate strength, complex stress test

1. Introduction

The complex geometric shapes of gas turbine engine parts and the loads acting on them lead to an inhomogeneous complex stress-strain state. The stress state can be estimated using the Lode-Nadai coefficient (1) [1,2] or the stress triaxiality factor (2) [3]:

$$\mu = 2\frac{\sigma_2 - \sigma_3}{\sigma_1 - \sigma_3} - 1, \quad (1)$$

$$\eta = -\frac{\sigma_0}{\sigma_i} - 1, \quad (2)$$

where σ_1, σ_2, and σ_3 are the principal stresses, σ_0 is the mean stress among the normal stresses or hydrostatic pressures, and σ_i is the stress intensity.

When parameters (1) and (2) at the nodes of the finite element model (FEM) of a modern turbine blade are calculated, large areas of the blade cover a complex stress state. Fig. 1 shows the distribution histograms of the Lode-Nadai coefficient at the nodes of the FEM of the blades with convective and perspective cooling systems, respectively.

Many criteria can quantitatively evaluate the complex stress state and the complex strain state. These criteria apply to various types of materials [4-6]. One of the main yield criteria studied by engineers is the criterion of maximum shear stress or the Tresca criterion (3) [7,8]. The yield criterion is as follows: plastic strains in the material occur when the maximum shear stress reaches its critical value.

$$\sigma_1 - \sigma_3 = \sigma_Y, \quad (3)$$

where σ_Y is the yield strength.

http://dx.doi.org/10.18149/MPM.4612020_17

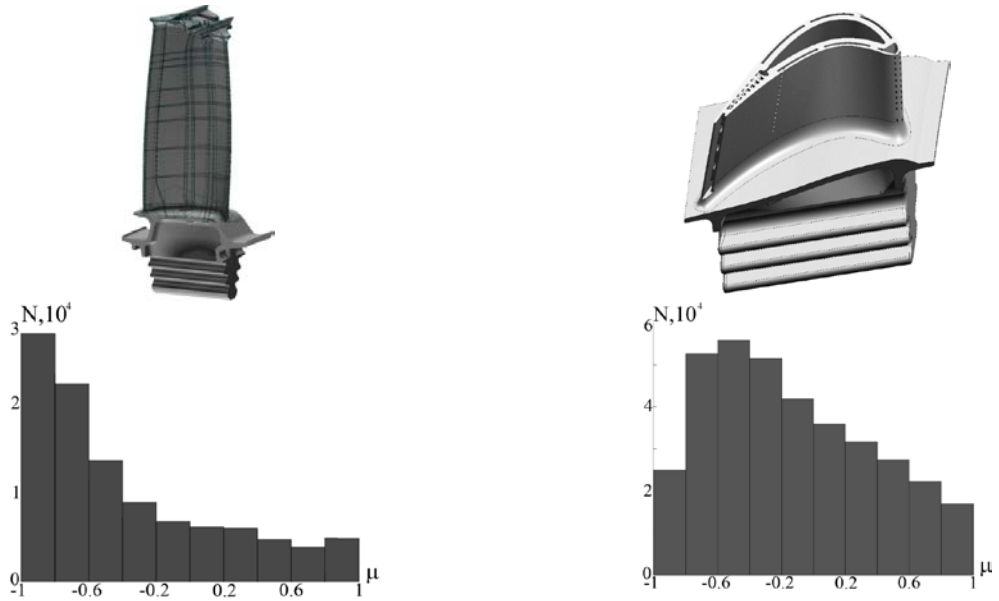

a) convective cooling system b) perspective cooling system

Fig. 1. Distribution histograms of the Lode-Nadai coefficient for the different blades

The next and most popular yield criterion is the von Mises criterion (4) [7,8]. This criterion is also called energetic because it is based on the potential energy of shape change.

$$\frac{1}{\sqrt{2}}\sqrt{(\sigma_1-\sigma_2)^2+(\sigma_2-\sigma_3)^2+(\sigma_3-\sigma_1)^2}=\sigma_Y. \quad (4)$$

Another criterion is called the Ishlinsky criterion (5) or the criterion of the greatest reduced stress. The reduced stress is the maximum among the normal components of the stress deviator.

$$max\{|\sigma_1-\sigma_0|,|\sigma_2-\sigma_0|,|\sigma_3-\sigma_0|\}=\frac{2}{3}\sigma_Y. \quad (5)$$

Currently, many yield criteria have been developed based on the systematization of experimental data, such as Mohr, Pisarenko-Lebedev, Hill, and Tsai-Wu [9,10]. If a criterion based on the systematization of experimental data is used, determining its coefficients from tests is required [e.g., Mohr's criterion (6) or the Pisarenko-Lebedev criterion (7)].

$$\sigma_1-\chi\sigma_3=\sigma_Y, \quad (6)$$

$$\chi\sigma_i+(1-\chi)\sigma_1=\sigma_Y, \quad (7)$$

where χ is the tensile/compressive yield strength ratio, σ_i – stress intensity.

Hill yield criterion is often used when stress-strain state calculations for anisotropic parts are performed.

$$F\left(\sigma_x-\sigma_y\right)^2+G\left(\sigma_y-\sigma_z\right)^2+H(\sigma_z-\sigma_x)^2+2L\tau_{xy}^2+2M\tau_{yz}^2+2N\tau_{zx}^2-\sigma_Y^2=0 \quad (8)$$

where $F=\frac{1}{2}\left(\frac{1}{R_x^2}+\frac{1}{R_y^2}-\frac{1}{R_z^2}\right)$, $G=\frac{1}{2}\left(\frac{1}{R_y^2}+\frac{1}{R_z^2}-\frac{1}{R_x^2}\right)$, $H=\frac{1}{2}\left(\frac{1}{R_z^2}+\frac{1}{R_x^2}-\frac{1}{R_y^2}\right)$, $L=\frac{3}{2}\left(\frac{1}{R_{xy}^2}\right)$, $M=\frac{3}{2}\left(\frac{1}{R_{yz}^2}\right)$, $N=\frac{3}{2}\left(\frac{1}{R_{zx}^2}\right)$, where $R_x=\frac{\sigma_x^Y}{\sigma_Y}$, $R_y=\frac{\sigma_y^Y}{\sigma_Y}$, $R_z=\frac{\sigma_z^Y}{\sigma_Y}$, $R_{xy}=\sqrt{3}\frac{\tau_{xy}^Y}{\sigma_Y}$, $R_{yz}=\sqrt{3}\frac{\tau_{yz}^Y}{\sigma_Y}$, $R_{zx}=\sqrt{3}\frac{\sigma_{zx}^Y}{\sigma_Y}$, σ_{ij}^Y – yield stress values.

When calculations are carried out for single-crystal (SX) parts considering the cubic symmetry of mechanical characteristics, Hill yield criterion is simplified and transformed into (9).

$$\sqrt{\left(\sigma_x-\sigma_y\right)^2+\left(\sigma_y-\sigma_z\right)^2+(\sigma_z-\sigma_x)^2+K_p(\tau_{xy}^2+\tau_{yz}^2+\tau_{zx}^2)}-\sigma_Y=0, \quad (9)$$

where $K_p = 4\frac{\sigma^2_{Y<001>}}{\sigma^2_{Y<011>}} - 1$, $\sigma_{Y<001>}$ – yield strength in <001> crystallographic direction, $\sigma_{Y<011>}$ – yield strength in <011> crystallographic direction. Further, it will become clear that in such formulation the criterion describes the material behavior worse than the Mises criterion. However, using the adjusted parameter ($K_p = 4\frac{\sigma^2_{Y<001>}}{\sigma^2_{Y<111>}} - 1$, where $\sigma^2_{Y<111>}$ – yield strength in <111> crystallographic direction) it is possible to achieve good agreement between theoretical and experimental data.

Based on Schmid's law [11] crystallographic approach is widely used for the stress-strain state determination of SX blades. According to Schmid's law, octahedral or cubic slip systems are realized when plastic deformation of the crystal lattice occurs.

$$\min_k\{n_k\}[\sigma]\{l_k\} > \tau_0, \tag{10}$$

where $\{n_k\}$ – the normal direction to the slip plane, $[\sigma]$ – stress tensor, $\{l_k\}$ – slip direction, τ_0 – critical resolved shear stress.

A.S. Semenov proposed an approach [12] to generalize the crystallographic criterion using smooth dependences based on the Hill yield criterion (11).

$$\left(\frac{I_{cs1}}{\sigma_Y}\right)^n + K_{p1}\left(\frac{I_{cs2}}{\sigma_Y}\right)^m - 1 = 0, \tag{11}$$

where $I_{cs1} = \sqrt{\frac{1}{2}\left[(\sigma_x - \sigma_y)^2 + (\sigma_y - \sigma_z)^2 + (\sigma_z - \sigma_x)^2\right]}$, $I_{cs2} = \sqrt{\tau^2_{xy} + \tau^2_{yz} + \tau^2_{zx}}$, K_{p1}, n, m – dimensionless material constants ($K_{p1} = 1.3$, $n = 2.4$, $m = 2.4$ [12]).

Studies show that no plasticity criterion can accurately describe the behavior of a material under a complex stress state. Different criteria are more consistent with the experimental data obtained from testing various materials and conditions.

In the present work, we focused on investigating SX material behavior under complex loading and a yield criterion based on the systematization of experimental data.

2. Experimental investigation

An experimental investigation of the yield criteria was conducted by testing thin-walled tubular specimens loaded by tensile/compressive force, and torque. In addition to the yield strength, several characteristics at various stress levels were studied. The stress state was assumed to be approximately plane.

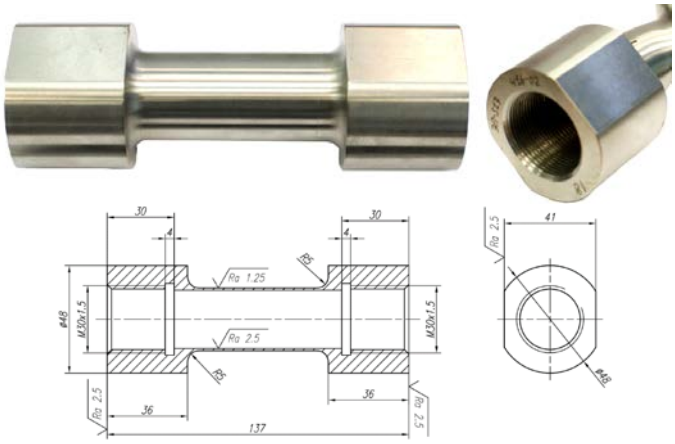

a) view of the specimen b) drawing of the specimen

Fig. 2. Thin-walled tubular specimen for testing under the complex stress state

SX specimens were cast so that the axis of the specimen matched with the crystallographic orientation (CO) <001> [13]. A drawing and view of the specimen are shown

in Fig. 2. A secondary orientation does not affect the general deformed state of axisymmetric specimens. Nevertheless, its search makes sense because SX materials are known to have a strong anisotropy of properties. Therefore, plastic strains could be unevenly distributed around the circumference of the specimens.

The test method corresponded with the requirements of regulatory documents [13]. The tests were conducted on a certified testing machine (Fig. 3). The testing machine works with tubular thin-walled specimens and is capable of loading them with tensile or compressive forces, torque, and internal pressure. However, in this work the specimens were not loaded by internal pressure.

Fig. 3. Testing machine POZ 0909 manufactured by Schenk GmbH (Germany) with a control system BiSS (India), a maximum tensile/compressive load of 630 kN, and a maximum torque of 8 kNm

The specimen was fixed in the testing machine using special equipment, excluding its slipping both at tension and at torsion. The tests were carried out under the control of the axial load and torque at a temperature of 20°C.

Strain gauges were used to measure the strains of the specimens. When a tension, compression, or torsion test is performed, conducting strain gauging becomes intuitively clear. However, if the stress state is complex, how to choose the angles for gluing on the specimen of the strain gauges is unclear. Strain gauges (Fig. 5) can measure only tensile or compressive strains. Thus, strain gauges are glued to the specimens in the directions where there are no shear strains (i.e., in the direction of the principal strains). The feature of isotropic materials is that normal stresses do not cause shear strains and that shear stresses do not cause tensile or compressive deformations. In this case, the directions of the principal stresses and principal deformations coincide, and determining these directions can be carried out according to a known stress state. Determining the principal stresses is a well-known eigenvalue problem described by Equation (12):

$$[\sigma - \lambda E]\{l\} = 0, \tag{12}$$

where σ is the stress tensor, λ is one of the principal stresses, and E is the unit tensor. If

relation (13) holds, the system (12) will have a solution.

$$det|\sigma - \lambda E| = 0. \quad (13)$$

The definition of the determinant leads to a cubic equation, the solution of which contains the eigenvalues or principal stresses. Then, the system of Equation (12) is solved given Equation (14):

$$l_1^2 + l_2^2 + l_3^2 = 1, \quad (14)$$

where l_1, l_2, l_3 are the directing cosines.

When SX specimens (anisotropic) are tested, tensile stresses can cause shear strains and vice versa. In this case, the directions of the principal stresses may differ from the directions of the principal strains, and recalculating the stresses into the strains is necessary using the generalized Hooke's law for an anisotropic material (15) [14]. Next, calculating the principal strains and their directions is necessary in the same way as in the stresses.

$$\{\varepsilon\} = [S]\{\sigma\}, \quad (15)$$

where $\{\varepsilon\}$ is the strain column vector, $[S]$ is the anisotropic compliance tensor, and $\{\sigma\}$ is the stress column vector.

In the beginning, we were faced with the issue of an unknown azimuthal orientation of the SX. The annular plates were cut from the end face of the specimen blanks (Fig. 4) and marked with marks on the cut and mating parts to identify the azimuthal orientation. The specimen blanks were sent for mechanical treatment, and the annular plates were sent for etching to identify the SX texture and determine the azimuthal CO. After etching and specimen fabrication, the separated parts were combined according to the previously identified marks. Thus, the azimuthal orientation of the SX in the specimens was determined.

Fig. 4. Annular plates after etching and the SX texture

The known azimuthal orientation of the SX shows how to recalculate the elastic tensor, as it depends on the orientation of the SX in the specimen, and to calculate the strain tensor. After determining the principal strains and their directions, the gluing of the strain gauge was conducted (Fig. 5).

The experimental design and yield strength values are presented in Table 1. Seven SX specimens were tested.

As a result of the tests, all specimens were destroyed in a brittle manner. Figure 6 shows the destroyed specimens after the tensile, compression, and torsion tests.

The following types of stress state were realized: uniaxial tension ($\sigma_1 = \sigma_{Ten}, \sigma_3 = 0$), uniaxial compression ($\sigma_3 = \sigma_{Com}, \sigma_1 = 0$), pure shear ($\sigma_1 = -\sigma_3$), and the combinations of tension–torsion and compression–torsion. The stress-strain diagram was obtained under a complex stress state in the coordinates of stress intensity–strain intensity. The yield strengths were calculated based on the fact that residual strains after unloading should not exceed 0.2% (Fig. 7a, black line).

Fig. 5. Specimen with strain gauges before torsion testing (principal strains are located at an angle of 45º to the axis of the specimen)

Table 1. The ratio of torque and tensile load when SX specimens were tested and experimental results

Number of points on the figure	Ratio of torque and tensile load $\left(\frac{M}{N}\right), \frac{\text{kN·mm}}{\text{kN}}$	Ratio of principal stresses $\left(\left\|\frac{\sigma_1}{\sigma_3}\right\|\right)$	Yield strength $(\sigma_{\text{Y}}), \text{MPa}$	Ultimate strength $(\sigma_{\text{u}}), \text{MPa}$
1	0	Inf.	873	960
2	7.57	3	952	1067
3	17.5	3/2	1219	1276
4	Inf.	1.0	1306	1368
5	-17.5	2/3	1415	1445
6	-7.57	1/3	1181	1235
7	-0	0	999	1029

Note: Sign «-» indicates that the specimen is under compression.

a) tension b) compression c) torsion

Fig. 6. Brittle destruction of specimens from SX alloy

To trace the evolution of plastic strains, the proportionality limit, the stresses at which residual strains were 0.1%, and the ultimate strength were determined. To determine the proportional limit, a black dashed line was used (Fig. 7a) (the tangent between the black dashed line and the abscissa axis is 50% less compared to Young's modulus). The stress-strain

diagram was compared to various types of stress states (Fig. 7b). These curves are clearly shown to be significantly different. This is explained by the anisotropy of the material and the fact that the modulus of elasticity and modulus of shear are not dependent quantities.

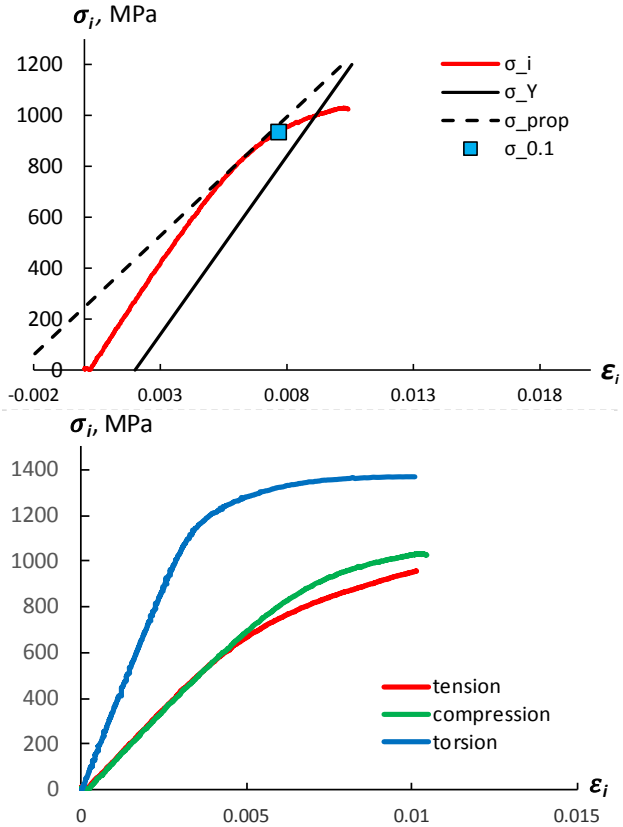

a) an example of the determination of some alloy characteristics

b) strain-stress curves for various types of stress states

Fig. 7. Stress-strain curves for the SX nickel-based alloy

The diagram for the dimensionless reference axis σ_1-σ_3 was obtained (Fig. 8a). An attempt was made to describe the experimental results using the most popular plasticity criteria [4-6,10-12]: Tresca yield criterion (3), von Mises (4), Pisarenko-Lebedev (7) Hill (8,9), Schmid (10), modified Hill criterion (11) and a modified Pisarenko-Lebedev yield criterion developed by the authors in (16).

$$\chi\sqrt{\frac{{\sigma_1}^2+\gamma\sigma_1\sigma_3+{\sigma_3}^2}{2}}+(1-\chi)\sigma_1=\sigma_Y, \tag{16}$$

where γ is the shear/tensile yield strength ratio. The values of constant of the proposed criterion:

$\sigma_Y = 873\ MPa$ (yield strength in <001> crystallographic direction), $\chi = 0.874$, $\gamma = 1.495$.

Credibility was evaluated (Table 2) using Equation (17) and (18) for various yield criteria. This value shows the accuracy of matching with the experimental data of one or another plasticity criterion.

$$K_{EC} = 1-\frac{\sum|y_i-\hat{y}_i|}{\sum|y_i|}, \tag{17}$$

$$R^2 = 1-\frac{\sum(y_i-\hat{y}_i)^2}{\sum(y_i-\bar{y})^2}, \tag{18}$$

where y_i is the experimental value of the yield strength, and $\hat{y}_i$ is the predicted value of the

yield strength, $\bar{y}$ is the average value among experimental data of yield strength.

Table 2. Evaluation of credibility of various yield criteria

Estimation criteria	Yield criteria							
	von Mises	Tresca	Pisarenko-Lebedev	Schmid's low	Hill	Hill (SX)	Power criterion	Modified Pisarenko-Lebedev
K_{EC}	78%	74%	83%	92%	94%	73%	94%	96%
R^2	-	-	-	-	41%	-	42%	75%

Most of the widely used yield criterion was not capable of describing the behavior of a given SX alloy. Therefore, the development of a modified criterion, which allows the reliable evaluation of the behavior of the material under complex stress–inelastic state, is required.

Based on the developed modified yield criterion, an attempt was made to trace the behavior of the material along the entire strain path (Fig. 8b). Four points were selected for each deformation curve: proportionality limit, stress at which the residual strain after unloading becomes 0.1%, yield strength, and ultimate stress limit. The behavior of the material changed depending on the type of stress state. The researched values and stress range between the proportionality limit and the ultimate stress limit changed, directly affecting the tangent modulus.

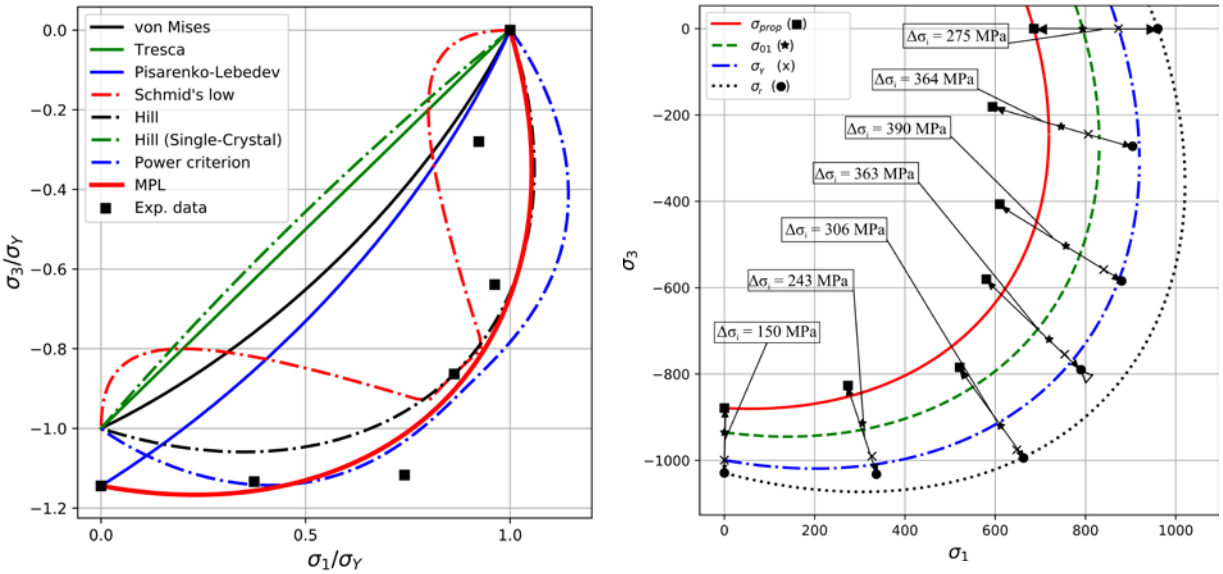

a) description of the yield strength using the popular yield criteria and the modified Pisarenko-Lebedev (MPL) yield criterion

b) description of several characteristics of the alloy using the modified Pisarenko-Lebedev plasticity criterion

Fig. 8. Diagrams of the characteristics of the SX alloy depending on the type of stress state

The approach proposed by the authors allows to describe the behavior of the material more accurately than previously developed approaches (Table 2 and Fig. 8a). Taking into account the tension–compression asymmetry of the material is an additional advantage of the proposed approach.

3. Conclusions

Test data analysis of specimens made from an SX nickel-based alloy, which were tested at various types of stress states at a temperature of 20°C, showed that the widely used yield

criteria of von Mises, Pisarenko-Lebedev, and Tresca were not able to reliably describe the behavior of the material under a complex stress state. A specialized criterion based on the systematization of experimental data was developed that could accurately describe the behavior of most materials. The type of stress state could affect the tangent modulus. In this case, the law of hardening of the material depends on the type of stress state.

This work may be further developed by conducting experimental studies on the alloy under complex stress conditions at elevated temperatures and tests under biaxial tension and their combination.

Acknowledgements. *No external funding was received for this study.*

References

[1] Lode W. Versuche ueber den Einfluss der mittleren Hauptspannung auf das Fliessen der Metalle Eisen. Kupfer und Nickel. *Z. Physik.* 1926:36: 913-939.

[2] Nadai A, Wahl AM. *Plasticity. A Mechanics of the Plastic State of Matter*. New York; 1931.

[3] Bao Y, Wierzbicki T. On fracture locus in the equivalent strain and stress triaxiality space. *Int. J. Mech. Sci.* 2004:46(1): 81-98.

[4] Kelly P. Solid mechanics part II: An introduction to solid mechanics. In: *Solid mechanics lecture notes*. University of Auckland. 2013. p.241-324.

[5] Mao-Hong Y, Guo-Wei M, Hong-Fu Q, Yong-Qiang Z. Basic Characteristics of Yield of Materials under Complex Stress. Springer. In: *Generalized Plasticity*. Berlin; 2006. p.33-49.

[6] Lei C, Weidong W, Haitao C. Yielding description for a Ni3Al based intermetallic alloy. *Materials and Design.* 2012:41: 192-197.

[7] Kachanov LM. *Fundamentals of fracture mechanics.* Moscow: Nauka; 1974. (In Russian)

[8] Malinin NN. *Applied theory of plasticity and creep*. Moscow: Mashinostroenie; 1975. (In Russian)

[9] Mujzemnek AY, Kartashova ED. *Mechanics of deformation and fracture of polymer resinous composite materials*. Penza: PGU; 2017. (In Russian)

[10] Hill R. *The Mathematical Theory of Plasticity.* New York: Oxford University Press; 1983.

[11] Shalin RE, Svetlov EB. *Single crystals of nickel heat-resistant alloys.* Moscow. Mashinostroenie; 1997. (In Russian)

[12] Semenov AS. Two-Invariant Power-Law Plasticity Criterion for Single Crystals of Cubic Symmetry. In: *Uprugost' i neuprugost'*. Moscow: Izdatel'skij Dom MGU imeni M.V. Lomonosova; 2016. p.250-255. (In Russian)

[13] State standard. GOST 25.502. *Methods for mechanical testing of metals. Fatigue Test Methods*. Moscow: Izdatelstvo standartov. 1986. (In Russian)

[14] Lekhnickij SG. *The theory of elasticity of an anisotropic body*. Moscow: Nauka; 1977. (In Russian)